Life Sciences 229 (2019) 46–56

Contents lists available at ScienceDirect

Life Sciences

journal homepage: www.elsevier.com/locate/lifescie

IL-17A-stimulated endothelial fatty acid β-oxidation promotes tumor angiogenesis

Ruirui Wang[a], Xiaohan Lou[a], Guang Feng[b], Jinfeng Chen[c], Linyu Zhu[a], Xiaomeng Liu[a], Xiaohan Yao[a], Pan Li[d], Jiajia Wan[a], Yi Zhang[e], Chen Ni[a,*], Zhihai Qin[a,f,*]

[a] Medical Research Center, the First Affiliated Hospital of Zhengzhou University, Zhengzhou, Henan Province 450052, China
[b] Department of Orthopedics, Zhengzhou Central Hospital, Zhengzhou, Henan Province 450052, China
[c] Research Center for Clinical System Biology, the First Affiliated Hospital of Zhengzhou University, Zhengzhou, Henan Province 450052, China
[d] Department of Pathology, the First Affiliated Hospital of Zhengzhou University, Zhengzhou, Henan Province 450052, China
[e] Biotherapy Center, the First Affiliated Hospital of Zhengzhou University, Zhengzhou, Henan Province 450052, China
[f] Key Laboratory of Protein and Peptide Pharmaceuticals, CAS-University of Tokyo Joint Laboratory of Structural Virology and Immunology, Institute of Biophysics, Chinese Academy of Sciences, University of the Chinese Academy of Sciences, Beijing, 100000, China

ARTICLE INFO

Keywords:
IL-17A
Angiogenesis
Mitochondrial respiration
FAO
AMPK

ABSTRACT

Aims: Tumor growth is an angiogenesis-dependent process that requires sustained new vessel growth. Interleukin-17 (IL-17A) is a key cytokine that modulates tumor progression. However, whether IL-17A affects the metabolism of endothelial cells is unknown.

Main methods: A xenograft model was established by implanting H460 (human lung cancer cell line) cells transfected with IL-17A-expressing or control vector. The effects of IL-17A on sprouting and tube formation of human umbilical vein endothelial cells (HUVECs) were measured. After treatment with IL-17A, the proliferation and migration of HUVECs were examined. Liquid chromatography-mass spectrometry (LC-MS) and Seahorse were used to detect the effects of IL-17A on mitochondrial respiration and fatty acid β-oxidation (FAO) in HUVECs. Western blotting was used to examine signaling pathways.

Key findings: Herein, we found that IL-17A promoted H460 tumor growth and angiogenesis *in vivo* and *in vitro*. Moreover, IL-17A stimulated angiogenesis by enhancing FAO, increasing mitochondrial respiration of endothelial cells. The AMP-activated protein kinase (AMPK) signaling pathway was activated to promote FAO. Finally, IL-17A-induced angiogenesis was blocked when FAO was inhibited using etomoxir.

Significance: In summary, these results indicate that IL-17A stimulates angiogenesis by promoting FAO. Thus, our study might provide a new therapeutic target for angiogenic vascular disorders.

1. Introduction

Sprouting angiogenesis is a complex process involving cell proliferation, migration and capillary-like tube formation [1], and the process of angiogenesis is closely related to cancer [2–5]. Tumor cells or stromal cells may cause imbalances that increase the elaboration of angiogenic inducers or decrease the production and effects of angiogenic suppressors. Therefore, the identification of endogenous angiogenesis stimulators or inhibitors is of great interest [2,6].

IL-17A is a major effector cytokine primarily derived from T helper 17 (Th17) cells [7]. Recently, it was reported that IL-17A is also secreted by several other cell types, including macrophages, nature killer T (NKT) cells, and neutrophils [8–12]. Although most IL-17A is derived from Th17 and other immune cells, the IL-17A receptor (primarily referred to as IL-17RA) is present in different cell types, including epithelial cells, endothelial cells and fibroblasts. The prevalence of IL-17RA expression may be responsible for IL-17A-mediated effects [13,14]. IL-17A mediates signaling through a novel ACT1-dependent pathway that ultimately activates pro-inflammatory factors, such as NF-κB [15]. IL-17A reportedly inhibits tumor cell apoptosis, impairs antitumor responses, and promotes tumor metastasis, invasion and angiogenesis [16–20]. Our previous work demonstrated that IL-17A promotes tumor progression by enhancing cancer stemness and angiogenesis [17,21]. Recently, Numasaki M et al. reported that IL-17A/F, which is a heterodimeric cytokine, directly promotes angiogenesis by promoting endothelial migration and tube formation [22].

* Corresponding authors at: Medical Research Center, The First Affiliated Hospital of Zhengzhou University, Zhengzhou University, NO. 1 Jianshe East Road, Zhengzhou, Henan 450052, China.
E-mail addresses: nichen904@163.com (C. Ni), zhihai@ibp.ac.cn (Z. Qin).

https://doi.org/10.1016/j.lfs.2019.05.030
Received 13 February 2019; Received in revised form 8 May 2019; Accepted 10 May 2019
Available online 11 May 2019
0024-3205/

Similarly, human retinal vascular endothelial cell (HREC) capillary tube formation is increased by IL-17A through enhancing endothelial migration, proliferation, and expression of VEGF, ICAM-1, IL-6 and IL-8 [23]. In addition, IL-17A induces the production of other angiogenic factors, including CXCL1, CXCL5 and CXCL8, by tumor cells to indirectly affect endothelial cells [24].

Targeting endothelial cells to inhibit pathological angiogenesis may be beneficial for patients with cancer. Endothelial metabolism is a novel target to treat angiogenesis and endothelial cell dysfunction [25]. Recent studies have shown that endothelial cells primarily rely on glycolysis for ATP production and biomass synthesis, which is necessary for key steps of angiogenesis, such as proliferation and migration [26]. However, upon glucose deprivation, glucose uptake was reduced, and energy production was shifted from glycolysis to mitochondrial respiration [27,28]. Indeed, mitochondria in endothelial cells have a high bioenergetic reserve capacity and can substantially increase respiration during stress conditions of glucose deprivation or oxidative stress [29,30]. When endothelial cells use mitochondrial respiration as their primary metabolic pathway, fatty acid β-oxidation (FAO) might be the main source of mitochondrial respiration [27,28]. Sandra Schoors et al. reported for the first time that FAO in endothelial cells was critical for vessel sprouting *in vivo*, and its role was more important than expected [28]. Overall, endothelial metabolism plays a key role in angiogenesis. Although IL-17A was reported to affect endothelial cells directly or indirectly, whether IL-17A affects endothelial cells by regulating mitochondrial respiration and FAO is unknown.

Our results indicated that IL-17A promotes angiogenesis by enhancing the FAO of endothelial cells. Reducing FAO using etomoxir blocked IL-17A-induced angiogenesis. These findings may provide a new target for angiogenic vascular disorders.

2. Materials and methods

2.1. Cell culture

Human umbilical vein endothelial cells (HUVECs) were kindly provided by Dr. Xiyun Yan. HUVECs were maintained in high-glucose Dulbecco's Modified Eagle's Medium (DMEM) supplemented with 10% fetal bovine serum (FBS), 100 units/mL penicillin, and 100 mg/mL streptomycin.

2.2. In vivo xenograft experiments

Animal protocols were approved by the Review Board of the First Affiliated Hospital of Zhengzhou University. Severe combined immunodeficient mice (female, 6 weeks old) were purchased from Vital River Laboratories (Beijing, China). In our previous work, we transfected H460 cells (human lung cancer cell line) with IL-17A-expressing or control vector [21]. In this study, the two transfected H460 cell lines (4×10^6) were resuspended in 100 μL PBS and injected into each mouse subcutaneously. Tumor growth was monitored every other day. Twenty-one days after cell transplantation, mice were sacrificed by cervical dislocation, and tumors were isolated for analysis ($n = 5$).

2.3. Immunofluorescence

Tumor tissues were harvested and embedded in paraffin. For histological staining of tumor tissues, paraffin sections were stained for rabbit-anti CD31 (1:100, NOVUS, #NB100–2284). The secondary antibody Dylight 555-conjugated goat anti-rabbit IgG (Thermo Fisher, #A21430) was used for immunofluorescence. Images were evaluated on a Perkin Elmer, Vectra machine.

2.4. Proliferation assay

HUVECs (3000 cells per well) dispensed in 200 μL culture medium per well were seeded into 96-well plates (Corning, #3559) and monitored at 4-h intervals using the IncuCyte live-cell imaging system (Essen Bio Science). Cells were stimulated with or without recombinant human IL-17A (rhIL-17A, 50 ng/mL, Peprotech, #200-17), IL-17RA inhibitor (IL-17RA Ab, 1.5 μg/mL, R&D, #MAB177), etomoxir (40 μM, Sigma-Aldrich, #E1905) and oligomycin (1 μM, Sigma-Aldrich, #O4876) when confluence reached 40%. Then, the cells were monitored by IncuCyte for 2 days without additional preparation. Cells placed in the IncuCyte were observed using phase microscopy and the 10× objective (Nikon, #MRH00101). Phase object confluence was calculated using IncuCyte analysis software ($n = 6$).

2.5. Migration assay

HUVECs (2×10^4 cells/well) were seeded into 96-well plates (Corning, #3559) and cultured overnight in the incubator. Scratch wounds were created using an IncuCyte wound maker when cell confluence was 90%. After washing, medium with or without rhIL-17A (50 ng/mL, Peprotech, #200-17), IL-17RA inhibitor (IL-17RA Ab, 1.5 μg/mL, R&D, #MAB177), etomoxir (40 μM, Sigma-Aldrich, #E1905) and oligomycin (1 μM, Sigma-Aldrich, #O4876) was added, and plates were placed inside the IncuCyte. Scratch areas were monitored over 24 h using the IncuCyte live-cell imaging system (Essen Bio Science) without additional preparation. Cells placed in the IncuCyte were observed using phase microscopy and the 10× objective (Nikon, #MRH00101). Relative wound density was calculated using IncuCyte analysis software ($n = 6$).

2.6. Tube formation assay

Ice-cold basement membrane matrix (Matrigel; Corning, #354234) was added at 60 μL per well into precooled 96-well plates and allowed to polymerize at 37 °C for 30 min. HUVECs (2×10^4 cells/well) treated with or without rhIL-17A (50 ng/mL, Peprotech, #8-17RA inhibitor (IL-17RA Ab, 1.5 μg/mL, R&D, #MAB177), etomoxir (40 μM, Sigma-Aldrich, #E1905) and oligomycin (1 μM, Sigma-Aldrich, #O4876) were plated onto the gel surface and incubated at 37 °C for 4 h ($n = 4$). Cell rearrangement and tube formation were visualized by microscopy (200×, Leica, DMi8, Germany).

2.7. Sprouting assay

Sprouting assays were performed as described [31]. Aortic rings were isolated from mice and embedded in Growth Factor Reduced Matrigel Matrix (Corning, #354230), supplemented with Primary Endothelial Cell Culture System (iCellBioscience, #PriMed-iCell-002), and 20% fetal bovine serum (FBS; PAA) with or without rhIL-17A (50 ng/mL, Peprotech, #200-17), etomoxir (40 μM, Sigma-Aldrich, #E1905) and oligomycin (1 μM, Sigma-Aldrich, #O4876) ($n = 4$–5). Endothelial sprouting was imaged 10 days after rings were seeded.

2.8. Glycolytic function assay

HUVECs (6000 per well) dispensed in 80 μL culture medium per well were seeded into XF96 Cell Culture Microplates (Agilent). After overnight culture, cells were treated with or without rhIL-17A (50 ng/mL, Peprotech, #200-17) for 24 h ($n = 6$). Culture medium was changed to XF Base Medium (Agilent, #102353-100) containing 2 mM L-glutamine (Sigma-Aldrich, #V900419) 1 h before beginning the assay. Glucose, oligomycin, and 2-DG (Seahorse XF Glycolysis Stress Test Kit; Agilent, #103020-100) were subsequently injected into the medium to final concentrations of 10 mM, 1 μM, and 50 mM, respectively. The extracellular acidification rate (ECAR) was measured using a Seahorse XF96 extracellular-flux analyzer (Agilent). Finally, we used Hoechst 33342 (Solarbio, #C0030) to normalize cell numbers following the manufacturer's instructions.

2.9. Glucose analog uptake

2-[N-(7-Nitrobenz-2-oxa-1,3-diaxol-4-yl)amino]-2-deoxyglucose (2-NBDG) is taken into cells through glucose transporters and phosphorylated by hexokinase. HUVECs (2×10^5 cells/well) were seeded in 24-well plates. After overnight culture, cells were treated with or without rhIL-17A (50 ng/mL, Peprotech, #200-17) for 24 h ($n = 5$). Then, the cells were washed with PBS, followed by the addition of low glucose culture media supplemented with 2-NBDG (100 μM, Life Technologies, #N13195) and incubated for 45 min at 37 °C. Then, the cells were harvested, centrifuged at 1500 rpm for 5 min at 4 °C, washed twice with ice-cold PBS and kept on ice. A control sample lacking 2-NBDG was used to set the flow cytometer compensation and gate parameters for 2-NBDG positive and negative events. Finally, cellular fluorescence was measured by flow cytometry.

2.10. Mitochondrial respiration

HUVECs (6000 per well) dispensed in 80 μL culture medium per well were seeded into XF96 Cell Culture Microplates (Agilent). After overnight culture, cells were treated with or without rhIL-17A (50 ng/mL, Peprotech, #200-17), IL-17RA inhibitor (IL-17RA Ab, 1.5 μg/mL, R &D, #MAB177) and Compound C (AMPK inhibitor, 5 μM, MCE, #HY-13418A) for 24 h ($n = 6$). The culture medium was changed to XF Base Medium (Agilent) 1 h before beginning the assay. Blockers were sequentially injected through the ports of the Seahorse Flux Pak cartridges. The oxygen consumption rate (OCR) was measured using a Seahorse XF96 extracellular flux analyzer (Agilent). OCR was normalized according to Hoechst 33342 (Solarbio, #C0030) staining. Blockers, oligomycin (1 μM, Sigma-Aldrich, #O4876), 2-[2-[4-(trifluoromethoxy) phenyl]hydrazinylidene]-propanedinitrile (FCCP; 0.5 μM, Sigma-Aldrich, #C2920) and antimycin A (AA; 0.5 μM, Sigma-Aldrich, #A8674), were used in combination with rotenone (Rot; 0.5 μM, Sigma, #R8875).

2.11. Adenosine triphosphate determination

HUVECs (2×10^5 cells/well) were seeded into 24-well plates. After overnight culture, cells were treated with or without rhIL-17A (50 ng/mL, Peprotech, #200-17) for 24 h ($n = 6$). Cells were harvested for adenosine triphosphate (ATP) level determination by using a colorimetric/fluorometric assay kit (Bio Vision, #K354–100) according to the manufacturer's instructions. Protein concentration was assessed using the BCA method.

2.12. Western blotting

Quantified protein lysates were measured with a Protein BCA Assay Kit (Thermo Fisher, #23228) according to the manufacturer's instructions. Protein lysates were resolved on SDS-PAGE gels, transferred onto nitrocellulose membranes, and immunoblotted with primary antibodies (overnight at 4 °C) followed by horseradish-peroxidase-coupled secondary antibodies for 1 h at room temperature. Bands were revealed using an ECL Western Blot Kit (CWBIO, #CW00495) and detected using a ChemiDoc MP Imaging System (Bio-Rad). The following primary antibodies were used: APOE (Abclonal, #A7798), COX5A (Abclonal, #A6437), p-AMPK (Cell Signaling Technology, #2535), AMPK (Cell Signaling Technology, #5831), ACT1 (absin, #abs117432), p-NF-kB (Cell Signaling Technology, #3033), NF-kB (Cell Signaling Technology, #8042), phospho-Acetyl-CoA Carboxylase (p-ACC, Cell Signaling Technology, #11818), Acetyl-CoA Carboxylase (ACC, Cell Signaling Technology, #3676), p-AKT (Cell Signaling Technology, #4060), AKT (Cell Signaling Technology, #2920), and β-actin (1:5000, Abclonal, #AC004). For western blotting, all primary antibodies were used at a 1:1000 dilution unless otherwise stated.

2.13. Fatty acid β-oxidation

HUVECs (6000 per well) in XF96 Cell Culture Microplates were cultured in XF Base Medium containing glucose (500 μM, Sigma-Aldrich, #V900392), GlutaMAX (1 mM, Thermo Fischer Scientific, #35030-061), carnitine (500 μM, Solarbio, #541-15-1) and 1% FBS ($n = 6$). Forty-five minutes before the assay, cell layers were washed with FAO Assay Medium (111 mM NaCl, 4.7 mM KCl, 1.25 mM CaCl2, 2 mM MgSO4, 1.2 mM NaH2PO4) supplemented with 2.5 mM glucose (Sigma-Aldrich, #V900392), 500 μM carnitine (Solarbio, #541-15-1), and 5 mM HEPES (Sigma-Aldrich, #H4034), pH 7.4. Cells were covered with 135 μL of FAO Assay Medium per well and incubated for 30 min at 37 °C without carbon-dioxide control. Fifteen minutes prior to starting the assay, etomoxir (ETO, an inhibitor of FAO; 40 μM, Sigma-Aldrich, #E1905) or vehicle was added to each well. Immediately before the assay, 30 μL XF palmitate-bovine serum albumin FAO substrate (Palm:BSA) or bovine serum albumin (BSA) was added to appropriate wells. Oligo (2.5 μg/mL, Sigma-Aldrich, #O4876), FCCP (1.6 μM, Sigma-Aldrich, #C2920), and AA (2 μM, Sigma-Aldrich, #A8674) in combination with Rot (4 μM, Sigma, #R8875) were sequentially injected into the culture, and oxygen consumption rates were determined as described above. Basal and maximal OCR alterations due to exogenous or endogenous FAO were calculated as previously described [32].

2.14. Protein digestion

HUVECs were treated with 50 ng/mL rhIL-17A for 6 or 24 h or remained untreated ($n = 3$). Total protein from harvested cells was extracted using RIPA, and concentrations were measured using the BCA method. Then, 250 μg of protein was precipitated by adding 3 x volume of chilled acetone at −20 °C for 3 h. After centrifugation, proteins were dissolved in 7 M guanidine hydrochloride (Yeasen, #60307ES76) and transferred to an ultrafiltration tube. Samples were then reduced with 1 M dithiothreitol (DTT) (Sigma-Aldrich, #43815) (60 min at 55 °C) and alkylated with 20 mM iodoacetamide (30 min in the dark at room temperature). After centrifugation, 100 μL of 50 mM ammonium bicarbonate (Merck, #1066-33-7) was added, and the samples were centrifuged again. After placing the ultrafiltration tube into a new receiver tube, 100 μL of 50 mM ammonium bicarbonate and 0.2 μg/μL of 25 μL trypsin were added and incubated at 37 °C overnight. Trypsin-digested peptides were acidified using 0.5% formic acid prior to LC–MS/MS.

2.15. LC–MS/MS analysis

The Eksigent 415 with Microflow system coupled with the Eksigent Analytical column (0.3 × 150 mm C18 ChromXP 3 μm) and trap column (0.3 mm, C18 ChromXP 5 μm) were used for all chromatographic separations. Both solvent A and loading buffer were composed of 2% (v/v) acetonitrile with 0.1% (v/v) formic acid. Solvent B was composed of 98% (v/v) acetonitrile with 0.1% (v/v) formic acid. Samples were loaded at a flow rate of 10 μl/min for 3 min with loading buffer and eluted from the analytical column at a flow rate of 5 μl/min in a mixture of solvent A and B with a linear gradient, 0–1 min, 3–9%B; 1–75 min, 9–35%B; 75–80 min, 35–50%B; and 80–81 min, 50–80%B. The column was regenerated by washing in 80% solvent B for 4 min and re-equilibrated in 5% solvent B for 5 min.

A hybrid Quadrupole Time-of-Flight TripleTOFs 6600 mass spectrometer (SCIEX) was used for both IDA (information-dependent acquisition) and SWATH-MS analyses. The ion source was operated with the following parameters: ISVF 5500; GS1 20; GS2 15; CUR 30; and TEM 350. The data acquisition mode in the information-dependent acquisition (IDA) experiments was set to obtain a high resolution TOF-MS scan over a mass range of 350–1500 *m/z*, followed by 100 to 1500 m/z for MS/MS scans of 50 ion candidates per cycle, operating the

instrument in high sensitivity mode. The selection criteria for parent ions included the intensity, where ions had to be > 150 cps, with a charge state between 2 and 4. The dynamic exclusion duration was set for 15 s. Collision-induced dissociation was triggered by rolling collision energy. The ion accumulation time was set to 200 ms (MS) and 50 ms (MS/MS).

Data acquired from the IDA experiments were used to construct 70 overlapping windows over the full mass range (350–1500 *m/z*) scan for SWATH MS-based acquisitions. An accumulation time of 40 ms was set for each fragment ion, resulting in a total duty cycle of 3.10 s.

2.16. Ion library generation for SWATH analysis

Combined data from the IDA experiments were used to generate an ion library (.group file) for SWATH analysis. It was searched against the human UniProt database in ProteinPilot 5.0 (Sciex) software utilizing the Paragon algorithms with the following parameters: identification Sample Type, iodoacetamide Cys Alkylation, trypsin digestion, thorough search effort and with FDR analysis [33]. The resulting protein pilot group file was used as the ion library file for all SWATH file processing and quantification.

2.17. SWATH acquisitions and processing

Approximately 16 μg aliquots of tryptic peptides were used for each injection. Three technical replicates were performed for each group. All files from SWATH experiments were processed with PeakView 2.0. The ion library for SWATH analysis was selected from the IDA experiment. A maximum number of 9999 proteins were imported with unlabeled sample type. The retention time (RT) of all twelve runs was aligned using 10 manually selected peptides with high intensity from 15 to 80 min of the run. The processing setting parameters were as follows: 6 peptides per protein, 6 transitions per peptide, 95% peptide confidence threshold, 1% false discovery rate threshold, and 5-min XIC extraction window with 75 ppm XIC width. After processing, the generated ion library and all individual SWATH files were uploaded. GSEA software was used to examine IL-17A enriched profiles and proteins.

2.18. Statistical analysis

Data are expressed as the mean ± SD or mean ± SEM. Statistical analysis using *t*-tests or two-way ANOVA was performed using GraphPad Prism software. Statistically significant differences are indicated as follows: *, $P < 0.05$; **, $P < 0.01$; ***$P < 0.001$.

3. Results

3.1. IL-17A promotes tumor growth and angiogenesis in vivo and in vitro

To assess the effects of IL-17A on tumor growth, a xenograft model was established by implanting H460 cells, which were transfected with IL-17A-expressing or control vector [21]. The results demonstrated that IL-17A promotes tumor growth and angiogenesis *in vivo* (Fig. 1A-B). In addition, the effects of IL-17A on endothelial cells *in vitro* were investigated. We isolated aortic rings from wild-type mice and cultured them with or without IL-17A in a Matrigel system *ex vivo*. The results showed that aortic rings produced significantly more vascular sprouts in the presence of IL-17A (Fig. 1C). Moreover, a Matrigel angiogenesis assay was used to explore the effect of IL-17A on tube formation. We found that IL-17A promoted HUVECs (Human Umbilical Vein Endothelial Cells) formation of tube-like structures *in vitro* (Fig. 1D). Consistent with these findings, tube formation promoted by IL-17A was blocked in the presence of an IL-17RA inhibitor (Fig. 1D). Further, HUVECs showed significantly enhanced migration in response to IL-17A stimulation (Fig. 1E). Inhibiting IL-17RA abrogated the IL-17A-induced migration of HUVECs (Fig. 1E). Finally, we assessed the effect of IL-17A on the proliferation of HUVECs. The results revealed that IL-17A significantly promoted the proliferation of HUVECs (Fig. 1F). To verify its specificity, IL-17RA was blocked to detect the effect of IL-17A on endothelial proliferation. The results showed that inhibition of IL-17RA reversed the IL-17A-induced proliferation of HUVECs (Fig. 1F). Taken together, these data demonstrate that IL-17A promotes angiogenesis both *in vivo* and *in vitro*.

3.2. IL-17A enhances endothelial mitochondrial respiration

Next, we investigated the mechanism of IL-17A in promoting angiogenesis. HUVECs were cultured with or without IL-17A for 24 h. Then, global metabolic changes were analyzed by performing liquid chromatography-mass spectrometry (LC-MS). Subsequent heatmap analysis revealed that glycolysis-related proteins were downregulated in response to IL-17A treatment (Fig. 2A). Previous studies have shown that endothelial cells primarily rely on glycolysis for ATP and biomass synthesis, which is necessary for proliferation and migration, key processes of angiogenesis [26]. However, upon glucose deprivation, mitochondrial function is enhanced to maintain energy requirements [27,28]. In our study, we found that IL-17A significantly reduced glycolysis and glucose uptake in HUVECs (Fig. 2B-C). Therefore, the effects of IL-17A on mitochondrial respiration were investigated. Heatmap analysis of proteomics revealed that IL-17A increased the levels of mitochondrial respiration-related proteins (Fig. 2D). Next, mitochondrial respiration affected by IL-17A was confirmed by seahorse. IL-17A significantly promoted maximal respiration of HUVECs (Fig. 2E). Notably, IL-17A strongly enhanced the spare respiratory capacity of HUVECs (Fig. 2E). This clearly indicates that the reserve energy capacity of HUVECs is the major target of IL-17A. The specific effect of IL-17A on endothelial mitochondrial respiration was confirmed by blocking the IL-17A receptor. Inhibiting IL-17RA abrogated IL-17A-enhanced mitochondrial respiration in HUVECs (Fig. 2E). Angiogenesis is an energy-dependent process. Therefore, ATP production in response to IL-17A stimulation was measured. The results showed that intracellular ATP levels were increased in response to IL-17A (Fig. 2F). Overall, IL-17A facilitates angiogenesis by enhancing endothelial mitochondrial respiration.

3.3. IL-17A upregulates FAO as the primary source of mitochondrial respiration

According to current studies, fatty acid metabolism appears to be the primary mitochondrial energetic pathway that supports angiogenic proliferation by generating ATP or providing carbons for *de novo* nucleotide synthesis required for DNA replication [27,34]. Gene set enrichment analysis of proteomics showed that IL-17A enhanced cellular lipid metabolic processes (Fig. 3A). Heatmap analysis revealed that IL-17A promoted the expression of fatty acid metabolism-related proteins (Fig. 3B). FAO results tested by seahorse showed that IL-17A primarily improved maximal oxygen consumption rate (OCR) changes due to endogenous FAO, while basal OCR did not change (Fig. 3C). The specific effect of IL-17A on endothelial FAO was confirmed by blocking the IL-17A receptor. Inhibiting IL-17RA abrogated IL-17A-enhanced endogenous FAO of HUVECs (Fig. 3D). IL-17A had no effect on exogenous FAO (Fig. 3E-F). This result implies that IL-17A primarily enhances spare respiratory capacity by increasing endogenous FAO. In summary, these data indicate that IL-17A primarily increases FAO as a source of mitochondrial respiration.

3.4. Inhibition of FAO abolishes IL-17A-induced angiogenesis

To investigate the effects of FAO on angiogenesis, IL-17A-stimulated aortic rings were treated with or without etomoxir or oligomycin, blockers of FAO and mitochondrial respiration, respectively. We found that IL-17A-increased sprouting was reduced by treatment with

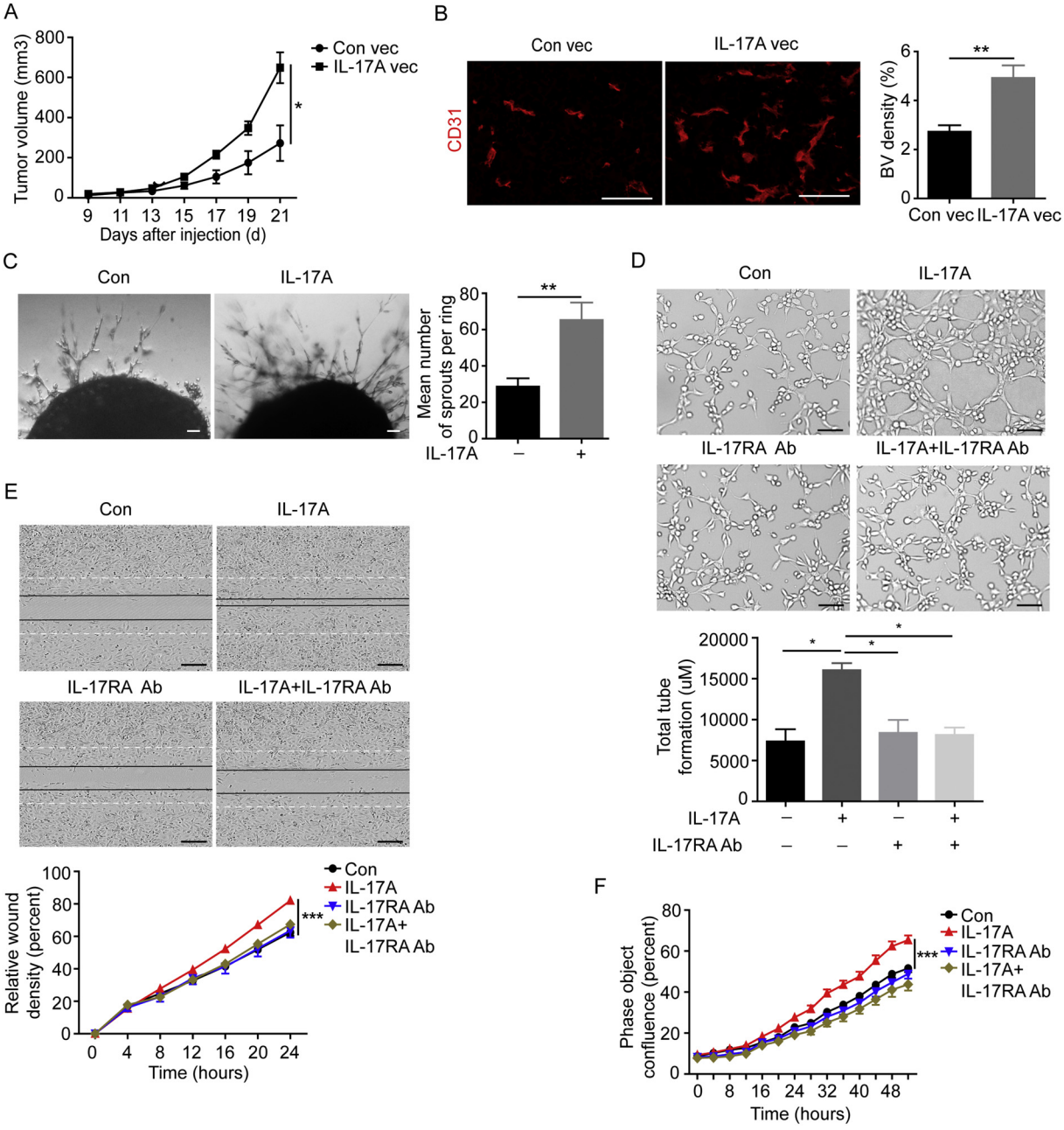

Fig. 1. IL-17A significantly promotes angiogenesis *in vivo* and promotes sprouts, tube formation, migration, and proliferation of HUVECs *in vitro*. (A) IL-17A promotes H460 tumor growth *in vivo*. IL-17A-expressing H460 (human lung cancer cell line) cells were injected subcutaneously into nude mice ($n = 5$). (B) IL-17A increases the density of $CD31^+$ tumor blood vessels *in vivo*. Tumor tissues were collected 21 days after cell implantation (n = 5). Tumor blood vessels were stained with CD31 antibody (red). Scale bar, 200 μm. (C) Representative results of sprouting assays of thoracic aortae. Thoracic aortic rings were embedded in Matrigel and cultured in the absence or presence of 50 ng/mL rhIL-17A for 10 days. Scale bar, 50 μm ($n = 4$–5). (D) Tube formation of HUVECs stimulated with or without rhIL-17A (50 ng/mL) and IL-17RA inhibitor (IL-17RA Ab, 1.5 μg/mL). Representative images were taken 4 h after treatment. Scale bar, 100 μm (n = 4). (E) Migration of HUVECs in the absence or presence of rhIL-17A (50 ng/mL) and IL-17RA inhibitor (IL-17RA Ab, 1.5 μg/mL). Representative micrographs of wound healing assays 0 and 20 h after creating a wound field. The percentage of relative wound density was calculated using IncuCyte. Scale bar, 100 μm ($n = 6$). (F) Proliferation of HUVECs (human umbilical vein endothelial cells) treated with or without rhIL-17A (50 ng/mL) and IL-17RA inhibitor (IL-17RA Ab, 1.5 μg/mL). The percentage of phase object confluence was calculated by using IncuCyte (n = 6). Values are shown as the mean ± SEM. * $P < 0.05$, ** $P < 0.01$, *** $P < 0.001$. (For interpretation of the references to color in this figure legend, the reader is referred to the web version of this article.)

etomoxir or oligomycin (Fig. 4A). Moreover, IL-17A-enhanced tube formation was abrogated by etomoxir or oligomycin administration (Fig. 4B). Furthermore, the migration of HUVECs, which was promoted by IL-17A, was reduced by treatment with etomoxir or oligomycin (Fig. 4C). Finally, IL-17A-induced proliferation of HUVECs was inhibited by treatment with oligomycin but not etomoxir (Fig. 4D). In conclusion, these results demonstrate that IL-17A promotes angiogenesis by enhancing FAO.

3.5. AMPK is activated to mediate IL-17A-enhanced FAO

Next, we verified the enzymes of FAO and mitochondrial respiration regulated by IL-17A. APOE is an apolipoprotein that plays an important role in lipid metabolism and mitochondrial function in the central nervous system, regulating neuron survival and sprouting [35]. COX5A transfers electrons from cytochrome *c* to oxygen during oxidative phosphorylation. IL-17A increases the expression of APOE and COX5A

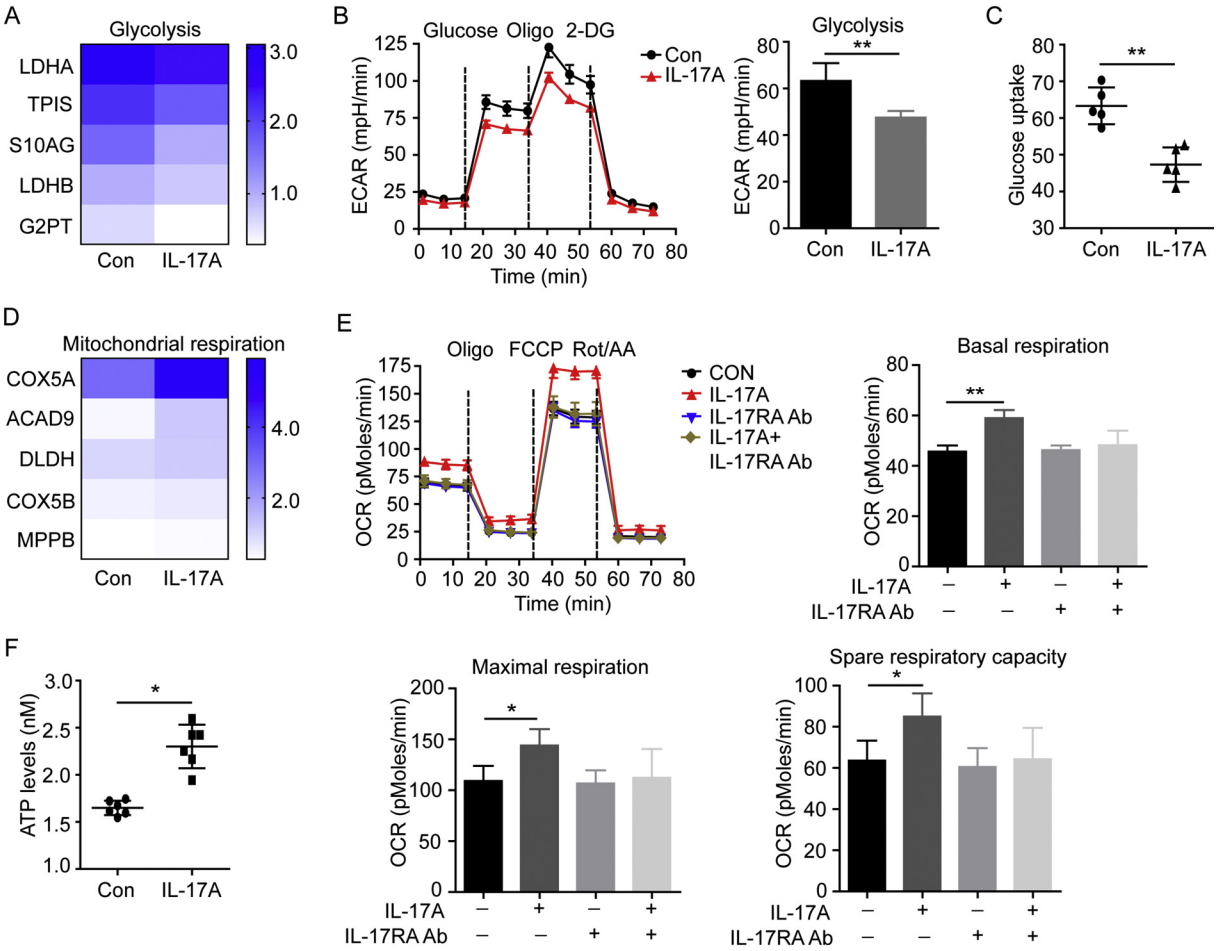

Fig. 2. IL-17A significantly promotes mitochondrial respiration of HUVECs. (A) Heatmap analysis of glycolytic panel protein levels in HUVECs that were treated with or without 50 ng/mL rhIL-17A ($n = 3$). Only those showing significant differences ($p < 0.05$) in expression level were selected for analysis. The color scale represents different expression ratios. (B) IL-17A downregulates the glycolytic function of HUVECs, as detected by the Seahorse Bioscience XF Analyzer. Six thousand cells/well were seeded into Seahorse plates. Cells were stimulated with or without 50 ng/mL rhIL-17A for 24 h ($n = 6$). (C) IL-17A reduces glucose uptake of HUVECs as measured by flow cytometry. Cells were stimulated with or without 50 ng/mL rhIL-17A for 24 h. 2-NBDG (100 μM) was incubated with cells for 30 min before cells were harvested ($n = 5$). (D) Heatmap analysis of mitochondrial respiration panel protein levels of HUVECs treated with or without 50 ng/mL rhIL-17A. Only those showing significant differences ($p < 0.05$) in expression level were selected for analysis. The color scale represents different expression ratios (n = 3). (E) HUVECs were treated with or without rhIL-17A (50 ng/mL) and IL-17RA inhibitor (IL-17RA Ab, 1.5 μg/mL) for 24 h. Mitochondrial respiration was measured using the Seahorse Bioscience XF Analyzer to assess basal respiration, maximal respiration, and spare respiratory capacity (n = 6). (F) HUVECs were treated with 50 ng/mL rhIL-17A for 24 h as indicated. Intracellular ATP levels were measured using a colorimetric/fluorometric assay kit (n = 6). Values are shown as the mean ± SD. * $P < 0.05$, ** $P < 0.01$.

(Fig. 5A). Previous results demonstrated that IL-17A enhances FAO. Therefore, the pathway that mediates the effects of IL-17A on FAO was investigated. AMPK activation was reported to accelerate β-oxidation of fatty acid [36,37]. In our study, IL-17A treatment activated AMPK phosphorylation (Fig. 5B). When IL-17RA was inhibited, IL-17A-induced phosphorylation of AMPK was inhibited (Fig. 5C). This result further demonstrated that IL-17A specifically activates the AMPK signaling pathway. To explore whether AMPK activation represents a new independent signaling pathway for angiogenesis or merely accompanies the profound inflammatory rearrangement of cellular metabolism orchestrated by Act1 and NF-κB, which comprise the classic downstream pathway of IL-17A, we assessed the effect of Act1/NF-κB on the AMPK pathway. Incubating cells with the NF-κB inhibitor did not affect IL-17A-induced phosphorylation of AMPK (Fig. 5D). These results suggest that AMPK activation is an independent signaling pathway for angiogenesis. Next, we investigated whether AMPK mediates the effects of IL-17A on FAO. The results showed that IL-17A-induced APOE and COX5A were reduced by an AMPK inhibitor (Fig. 5E). Subsequently, IL-17A-induced maximal respiration and spare respiratory capacity of HUVECs were blocked by an AMPK inhibitor (Fig. 5F). Thus, AMPK signaling mediates the promotion of IL-17A on FAO.

4. Discussion

Our studies are the first to demonstrate that FAO is upregulated by IL-17A in HUVECs. The principal findings of this study are as follows: (1) IL-17A significantly stimulates sprouting, tube formation, migration and proliferation of endothelial cells *in vitro* and angiogenesis in a xenograft model. (2) IL-17A mediates these effects by enhancing endothelial mitochondrial respiration, especially for FAO. (3) This system is regulated by AMPK signaling.

Consistent with our previous findings, IL-17A promoted H460 tumor growth and angiogenesis *in vivo* [21]. Our study further found that IL-17A enhanced sprouting, tube formation, migration and proliferation of HUVECs *in vitro*. Because neovascularization is a critical process for the sustained growth of solid tumors, our results suggest that IL-17A might accelerate tumor growth *via* promotion of angiogenesis. Other investigators have also confirmed that IL-17A facilitates angiogenesis in different tumor models. Moneo Numasaki et al. reported that IL-17A promotes angiogenesis in fibrosarcoma as well as in

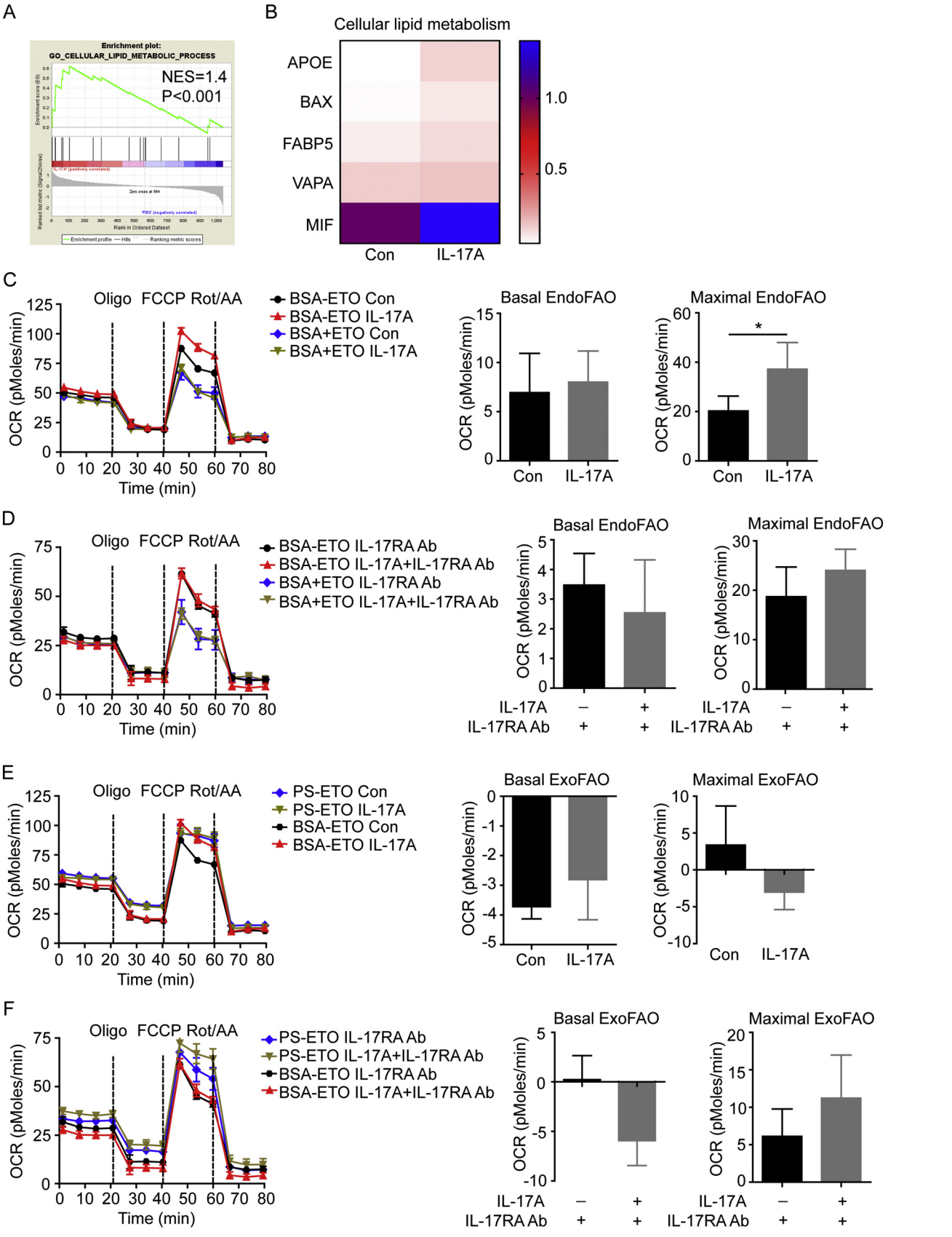

(caption on next page)

Fig. 3. IL-17A enhances the FAO of HUVECs. (A) Gene enrichment analysis by GSEA showed that IL-17A activated cellular lipid metabolism. NES, normalized enrichment score. The *P*-value represents a normal *p*-value ($n = 3$). (B) Heatmap analysis showed that FAO (fatty acid β-oxidation)-related proteins were upregulated in response to rhIL-17A (50 ng/mL) treatment. Only those showing significant differences ($p < 0.05$) in expression level were selected for analysis. Blue and red represent up- and downregulation, respectively (n = 3). (C–F) HUVECs were treated with or without rhIL-17A (50 ng/mL) and IL-17RA inhibitor (IL-17RA Ab, 1.5 μg/mL) for 24 h. Cultures that received or did not receive ETO, Palm:BSA and BSA prior to the addition of inhibitors of oxygen consumption were used to evaluate FAO. Basal and maximal OCR alterations due to exogenous or endogenous FAO were calculated. EndFAO, endogenous FAO; ExoFAO, exogenous FAO. Vertical dashed lines indicate the addition of the indicated blockers ($n = 6$). Values are shown as the mean ± SEM. * $P < 0.05$. (For interpretation of the references to color in this figure legend, the reader is referred to the web version of this article.)

colon adenocarcinoma [38]. They also showed that the IL-17A/F heterodimer promotes angiogenesis [22]. Seon Hee Chang et al. demonstrated that lack of IL-17A reduces angiogenesis in lung cancer [39]. QiongYing Lv et al. reported that IL-17A and HPSE might promote tumor angiogenesis and cell proliferation and invasion in cervical cancer [20].

Nearly 90,000 papers have been published on angiogenesis. In contrast, a limited number (<100) of publications have focused on the metabolic adaptations that are associated with the angiogenic switch or the possible implications for therapeutic (anti)-angiogenesis [25]. IL-17A promotes angiogenesis by enhancing the migration, proliferation and tube formation of endothelial cells or by increasing the expression of VEGF, ICAM-1, IL-6 and IL-8 in endothelial cells [22,23]. However, the effect of IL-17A on endothelial cell metabolism has not been elucidated. Previous studies have shown that endothelial cells primarily rely on glycolysis for ATP and biomass synthesis, which is necessary for the key processes of angiogenesis, such as proliferation and migration [26]. However, upon glucose deprivation or under conditions of stress, mitochondrial function is enhanced, and FAO might be the primary source to maintain energy requirements [27,28]. In our study, we found that IL-17A significantly reduced glycolysis and glucose uptake, which might explain why IL-17A increases mitochondrial respiration and FAO in HUVECs. However, the reason for IL-17A decreasing glucose uptake is unknown and needs further study. Our results showed that IL-17A promoted mitochondrial respiration primarily by increasing the spare respiratory capacity of HUVECs, which substantially improved respiration in stress conditions of glucose deprivation [30]. Mitochondrial respiration provides the basal energy required for normal metabolism and holds in reserve the potential for maximal respiration if required. This potential, the so-called spare respiratory capacity, serves the increased energy demand for maintaining cellular functions under stress [40,41]. However, whether mitochondrial biogenesis influences vascular sprouting and the specific mechanisms whereby this occurs need more in-depth studies. Although mitochondrial respiration can use glucose, glutamine and fatty acids as energy sources, FAO might be the primary mitochondrial energetic pathway to support angiogenic activities according to current research [28]. The possible reasons for this might include the following: first, FAO is the most efficient way to generate energy when mitochondrial respiration is the primary source of energy. Second, when endothelial cells use mitochondrial respiration as their main metabolic pathway, they may be in experiencing glucose deprivation. Additional reasons still need to be explored. In our study, FAO was enhanced to sustain IL-17A-induced mitochondrial respiration. Next, we explored the effects of endothelial metabolism, especially FAO, on IL-17A-induced angiogenesis. The results showed that both blocking endothelial FAO and mitochondrial respiration abrogated IL-17A-promoted angiogenesis. Interestingly, the effects of blocking FAO on angiogenesis were comparable to that of the control group, while the inhibition of angiogenesis by blocking mitochondrial respiration was stronger than that of the control group. Inhibiting mitochondrial respiration both reversed IL-17A-promoted angiogenesis and basal levels of angiogenesis. Blcoking FAO only reduced IL-17A-increased angiogenesis but not basal levels of angiogenesis. This results may indicate that FAO sustains IL-17A-enhanced angiogenesis. These results further demonstrate that IL-17A promotes angiogenesis by enhancing FAO. In addition, we found that inhibiting FAO using etomoxir reversed IL-17A-induced endothelial sprouting, tube formation, and migration but not proliferation. These results suggest that enhanced FAO sustains IL-17A-induced endothelial migration during angiogenesis but not proliferation. This is distinct from the study of Sandra Schoors, which reported that lack of CPT1A, a rate-limiting enzyme of FAO, caused vascular sprouting defects due to impaired proliferation, not migration, of human and murine endothelial cells [28]. This difference might be due to the different environment in which endothelial cells were located. In the study of Sandra Schoors, the environment in which endothelial cells were located was a normal physiological environment. However, in our study, endothelial cells were under the stress of inflammatory stimulation. Endothelial cells may need to change rapidly to deal with the stress. The migration of endothelial cells may be able to respond more rapidly to environmental changes than to proliferation. The mechanisms of FAO affecting angiogenesis require further study. IL-17A-induced endothelial proliferation may be due to other factors that are independent of FAO.

AMPK is thought to be a key modulator of the cellular response to ischemia and other stresses. Zeina Dagher et al. reported that FAO was increased by incubating HUVECs with AICAR, which stimulated AMPK signaling [42]. AMPK was also shown to play a key role in VEGF-mediated proliferation, migration and fatty acid metabolism of endothelial cells [43]. In our study, we found that IL-17A induced the phosphorylation of AMPK by binding with IL-17RA. Inhibiting AMPK abrogated IL-17A-enhanced FAO. IL-17RA activates the Act1/NF-κB cellular signal pathways [15]. Our results also confirmed that IL-17A activates the Act1/NF-κB signaling axis. NF-κB can either promote or repress oxidative phosphorylation and the switch to glycolytic energy production [44–46]. For example, Mauro et al. demonstrated that the NF-κB-dependent metabolic pathway involves stimulation of oxidative phosphorylation through upregulation of mitochondrial synthesis of cytochrome *c* oxidase 2 [45]. In contrast, TNFα-induced classical NF-κB activation enhances muscle glycolytic metabolism [46]. To identify whether AMPK activation represents a new independent signaling pathway for angiogenesis that not merely accompanies the profound inflammatory rearrangement of cellular metabolism orchestrated by Act1 and NF-κB, we detected the effect of Act1/NF-κB on the AMPK pathway. Our results demonstrated that when incubated with an NF-κB inhibitor, IL-17A still activates AMPK signaling. Indeed, AMPK activation was reported to suppress pro-inflammatory and enhance anti-inflammatory reactions [47–49]. For example, AICAR (an analogue of AMP) attenuated LPS-induced activation of NF-κB and inhibited expression of proinflammatory cytokines (TNFα, IL1β, IL-6) and iNOS [48]. These data indicate that AMPK is an independent pathway for angiogenesis rather than a concomitant phenomenon of deep inflammatory rearrangement on cellular metabolism coordinated by Act1 and NF-κB. Considering all these results, HUVECs enhance mitochondrial function in an AMPK-dependent manner when stimulated by IL-17A. This suggests that AMPK plays an important role in regulating FAO to increase angiogenesis-related functions.

Overall, our findings provide evidence that FAO plays a dominant role in IL-17A-induced angiogenesis. This is the first time that the mechanism of the IL-17A signaling pathway based on mitochondria has been demonstrated, especially for FAO. It is of great significance and may provide new mechanistic insights for angiogenic vascular disorders.

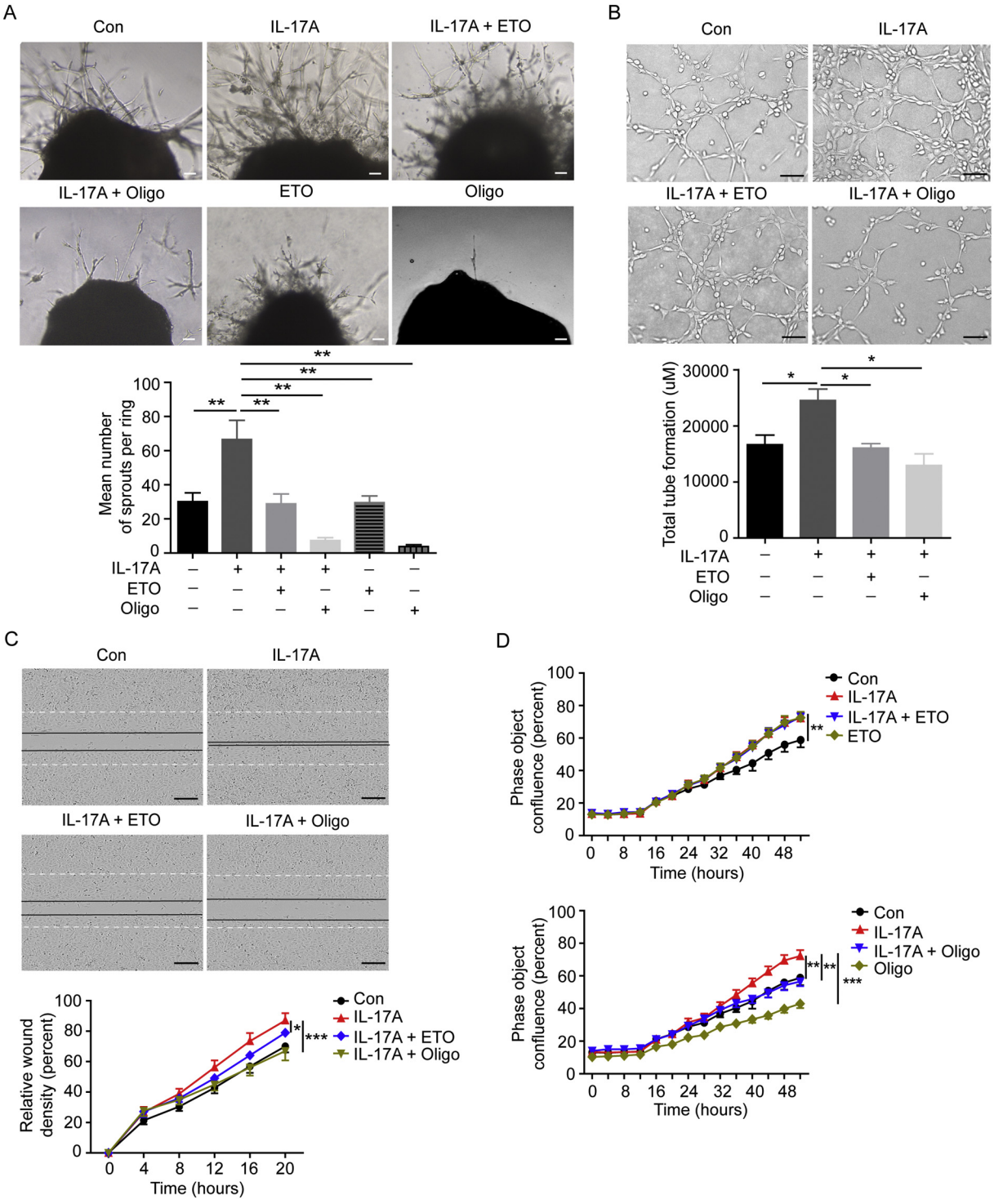

Fig. 4. Blocking FAO reverses IL-17A-induced sprouts, tube formation and migration of HUVECs *in vitro*. (A) Representative results of sprouting assays of thoracic aortae. Thoracic aortic rings were embedded in Matrigel and cultured in the absence or presence of rhIL-17A (50 ng/mL), ETO (40 μM) or oligomycin (1 μM) for 10 days. Scale bar, 50 μm (n = 4–5). (B) Tube formation of HUVECs stimulated with or without rhIL-17A (50 ng/mL), ETO (40 μM) or oligomycin (1 μM). Scale bar, 100 μm (n = 4). (C) Migration of HUVECs in the presence or absence of rhIL-17A (50 ng/mL), ETO (40 μM) or oligomycin (1 μM) was assessed by IncuCyte. Representative micrographs of migration assays at 0 and 20 h after creating a wound field. The percentage of relative wound density was calculated using IncuCyte. Scale bar, 100 μm (n = 6). (D) Proliferation of HUVECs treated with or without rhIL-17A (50 ng/mL), ETO (40 μM) or oligomycin (1 μM) was assessed by IncuCyte. The percentage of phase object confluence was calculated using IncuCyte (n = 6). Values are shown as the mean ± SEM. * $P < 0.05$, ** $P < 0.01$, *** $P < 0.001$.

5. Conclusions

In conclusion, we found that IL-17A stimulates angiogenesis by enhancing FAO in HUVECs. The promotion of FAO by IL-17A is dependent on AMPK activation. We are the first to show that FAO mediates IL-17A-induced angiogenesis. Thus, our study might provide a new target for angiogenic vascular disorders.

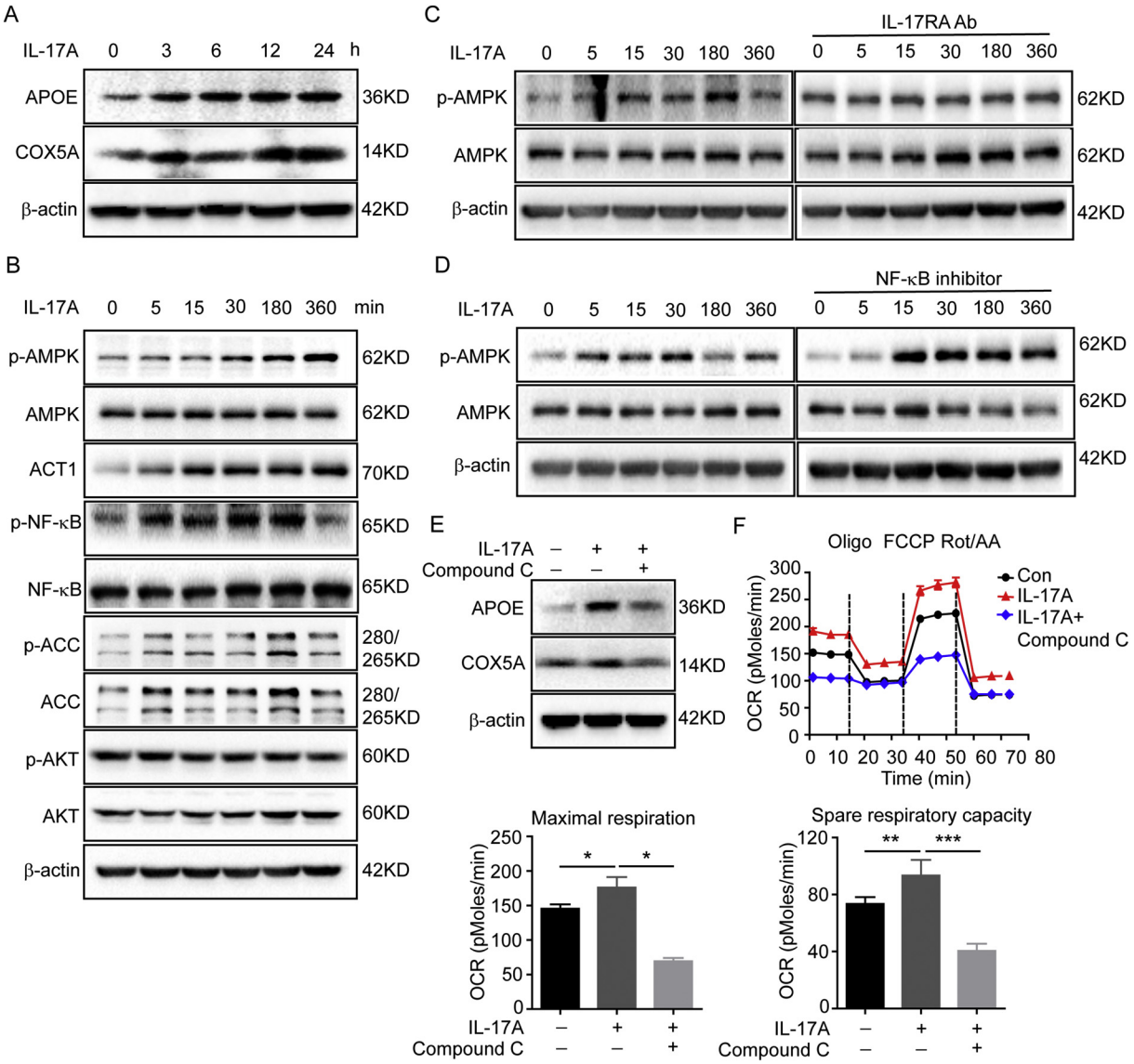

Fig. 5. IL-17A activates AMPK signaling to promote FAO. (A) Expression of APOE and COX5A in IL-17A-stimulated HUVECs was measured by western blot. (B) HUVECs were treated with or without rhIL-17A (50 ng/mL). Protein levels and phosphorylation states of AMPK (AMP-activated protein kinase), NF-κB, ACC, AKT and ACT1 were assessed by western blot. (C) Expression of AMPK in HUVECs treated with or without rhIL-17A (50 ng/mL) and IL-17RA inhibitor (IL-17RA Ab, 1.5 μg/mL) was measured by western blot. (D) Expression of AMPK in HUVECs treated with or without rhIL-17A (50 ng/mL) and NF-κB inhibitor (SC75741, 10 μM, Selleck, #S7273) was measured by western blot. (E) Expression of APOE and COX5A in HUVECs treated with or without rhIL-17A (50 ng/mL) and Compound C (5 μM) was measured by western blot. (F) HUVECs were treated with or without rhIL-17A (50 ng/mL) and Compound C (5 μM) for 24 h. Mitochondrial respiration was measured using the Seahorse Bioscience XF Analyzer by assessing basal respiration, maximal respiration, and spare respiratory capacity ($n = 6$). Values are shown as the mean ± SD. * $P < 0.05$, ** $P < 0.01$, *** $P < 0.001$.

Funding

This work was supported by the National Natural Science Foundation of China (81630068, 31670881 to Zhihai Qin) and the Health Commission of Henan Province (201601005 to Zhihai Qin).

Acknowledgments

We thank Erben Ulrike, Yangyang Bian and Ming Wang for their excellent technical assistance and helpful discussions. We thank Xixi Duan and Lijing Zhang for assistance with the experiments. This work was supported by the National Natural Science Foundation of China (81630068, 31670881 to Zhihai Qin) and the Health Commission of Henan Province (201601005 to Zhihai Qin).

Author contribution statement

Ruirui Wang performed most of the experiments. Xiaohan Lou, Jinfeng Chen, Xiaomeng Liu, Xiaohan Yao, Pan Li and Jiajia Wan performed some of the experiments or contributed to their design. Ruirui Wang, Guang Feng, Chen Ni and Zhihai Qin analyzed the data and drafted the manuscript. Chen Ni, Linyu Zhu, Yi Zhang and Zhihai Qin revised the manuscript. Ruirui Wang and Zhihai Qin finalized the paper. Zhihai Qin supervised the study. All authors were involved in writing the paper and had final approval of the submitted and published version.

Declaration of Competing Interests

The authors declare no conflicts of interest.

References

[1] J. Folkman, Tumor angiogenesis: therapeutic implications, N. Engl. J. Med. 285 (21) (1971) 1182–1186, https://doi.org/10.1056/NEJM197111182852108.

[2] J. Folkman, Seminars in medicine of the Beth Israel hospital, Boston. Clinical applications of research on angiogenesis, N. Engl. J. Med. 333 (26) (1995) 1757–1763, https://doi.org/10.1056/NEJM199512283332608.

[3] W.W. Li, V.W. Li, M. Hutnik, A.S. Chiou, Tumor angiogenesis as a target for dietary cancer prevention, J. Oncol. 2012 (2012) 879623, , https://doi.org/10.1155/2012/879623.

[4] S. Wang, Z. Xiao, Z. Hong, H. Jiao, S. Zhu, Y. Zhao, J. Bi, J. Qiu, D. Zhang, J. Yan, et al., FOXF1 promotes angiogenesis and accelerates bevacizumab resistance in colorectal cancer by transcriptionally activating VEGFA, Cancer Lett. 439 (2018) 78–90, https://doi.org/10.1016/j.canlet.2018.09.026.

[5] X. Zhao, M. Mohaupt, J. Jiang, S. Liu, B. Li, Z. Qin, Tumor necrosis factor receptor 2-mediated tumor suppression is nitric oxide dependent and involves angiostasis, Cancer Res. 67 (9) (2007) 4443–4450, https://doi.org/10.1158/0008-5472.CAN-07-0185.

[6] D. Ribatti, R. Tamma, Hematopoietic growth factors and tumor angiogenesis, Cancer Lett. 440-441 (2019) 47–53, https://doi.org/10.1016/j.canlet.2018.10.008.

[7] W. Jin, C. Dong, IL-17 cytokines in immunity and inflammation, Emerg. Microbes Infect. 2 (9) (2013) e60, https://doi.org/10.1038/emi.2013.58.

[8] X. Zhu, L.A. Mulcahy, R.A. Mohammed, A.H. Lee, H.A. Franks, L. Kilpatrick, A. Yilmazer, E.C. Paish, I.O. Ellis, P.M. Patel, et al., IL-17 expression by breast-cancer-associated macrophages: IL-17 promotes invasiveness of breast cancer cell lines, Breast Cancer Res 10 (6) (2008) R95, https://doi.org/10.1186/bcr2195.

[9] J.M. Coquet, S. Chakravarti, K. Kyparissoudis, F.W. McNab, L.A. Pitt, B.S. McKenzie, S.P. Berzins, M.J. Smyth, D.I. Godfrey, Diverse cytokine production by NKT cell subsets and identification of an IL-17-producing CD4-NK1.1- NKT cell population, Proc. Natl. Acad. Sci. U. S. A. 105 (32) (2008) 11287–11292, https://doi.org/10.1073/pnas.0801631105.

[10] L. Garcia-Hernandez Mde, H. Hamada, J.B. Reome, S.K. Misra, M.P. Tighe, R.W. Dutton, Adoptive transfer of tumor-specific Tc17 effector T cells controls the growth of B16 melanoma in mice, J. Immunol 184 (8) (2010) 4215–4227, https://doi.org/10.4049/jimmunol. 0902995.

[11] S. Punt, G.J. Fleuren, E. Kritikou, E. Lubberts, J.B. Trimbos, E.S. Jordanova, A. Gorter, Angels and demons: Th17 cells represent a beneficial response, while neutrophil IL-17 is associated with poor prognosis in squamous cervical cancer, Oncoimmunology 4 (1) (2015) e984539, , https://doi.org/10.4161/2162402X.2014.984539.

[12] Z. Yang, B. Zhang, D. Li, M. Lv, C. Huang, G.X. Shen, B. Huang, Mast cells mobilize myeloid-derived suppressor cells and Treg cells in tumor microenvironment via IL-17 pathway in murine hepatocarcinoma model, PLoS One 5 (1) (2010) e892, , https://doi.org/10.1371/journal.pone.0008922.

[13] L. Wei, H. Xiong, W. Li, B. Li, Y. Cheng, Upregulation of IL-6 expression in human salivary gland cell line by IL-17 via activation of p38 MAPK, ERK, PI3K/Akt, and NF-κB pathways[J], J. Oral Pathol. Med 47 (9) (2018) 847–855, https://doi.org/10.1111/jop.12765.

[14] C. Gu, L. Wu, X. Li, IL-17 family: cytokines, receptors and signaling[J], Cytokine 64 (2) (2013) 477–485, https://doi.org/10.1016/j.cyto.2013.07.022.

[15] S.L. Gaffen, Structure and signalling in the IL-17 receptor family[J], Nat. Rev. Immunol. 9 (8) (2009) 556–567, https://doi.org/10.1038/nri2586.

[16] X. Qian, H. Chen, X. Wu, L. Hu, Q. Huang, Y. Jin, Interleukin-17 acts as double-edged sword in anti-tumor immunity and tumorigenesis, Cytokine 89 (2017) 34–44, https://doi.org/10.1016/j.cyto.2015.09.011.

[17] M. Xiao, C. Wang, J. Zhang, Z. Li, X. Zhao, Z. Qin, IFNγ promotes papilloma development by up-regulating Th17-associated inflammation, Cancer Res 69 (5) (2009) 2010–2017, https://doi.org/10.1158/0008-5472.CAN-08-3479.

[18] B. Darvishi, A.K. Majidzadeh, R. Ghadirian, M. Mosayebzadeh, L. Farahmand, Recruited bone marrow derived cells, local stromal cells and IL-17 at the front line of resistance development to anti-VEGF targeted therapies, Life Sci 217 (2019) 34–40, https://doi.org/10.1016/j.lfs.2018.11.033.

[19] L. Wang, T. Yi, M. Kortylewski, D.M. Pardoll, D. Zeng, H. Yu, IL-17 can promote tumor growth through an IL-6-Stat3 signaling pathway[J], J. Exp. Med 206 (7) (2009) 1457–1464, https://doi.org/10.1084/jem.20090207.

[20] Q. Lv, K. Wu, F. Liu, W. Wu, Y. Chen, W. Zhang, Interleukin17A and heparanase promote angiogenesis and cell proliferation and invasion in cervical cancer[J], Int. J. Oncol 53 (4) (2018) 1809–1817, https://doi.org/10.3892/ijo.2018.4503.

[21] R. Wang, L. Yang, C. Zhang, R. Wang, Z. Zhang, Q. He, X. Chen, B. Zhang, Z. Qin, L. Wang, et al., Th17 cell-derived IL-17A promoted tumor progression via STAT3/NF-κB/Notch1 signaling in non-small cell lung cancer, Oncoimmunology 7 (11) (2018) e1461303, , https://doi.org/10.1080/2162402X.2018.1461303.

[22] M. Numasaki, H. Tsukamoto, Y. Tomioka, Y. Nishioka, T. Ohrui, A heterodimeric cytokine, consisting of IL-17A and IL-17F, promotes migration and capillary-like tube formation of human vascular endothelial cells, Tohoku J. Exp. Med 240 (1) (2016) 47–56, https://doi.org/10.1620/tjem.240.47.

[23] G. Liu, H. Wu, L. Chen, J. Xu, M. Wang, D. Li, P. Lu, Effects of interleukin-17 on human retinal vascular endothelial cell capillary tube formation in vitro[J], Mol. Med. Rep 16 (1) (2017) 865–872, https://doi.org/10.3892/mmr.2017.6623.

[24] M. Numasaki, M. Watanabe, T. Suzuki, H. Takahashi, A. Nakamura, F. McAllister, T. Hishinuma, J. Goto, M.T. Lotze, J.K. Kolls, et al., IL-17 enhances the net angiogenic activity and in vivo growth of human non-small cell lung cancer in SCID mice through promoting CXCR-2-dependent angiogenesis, J. Immunol 175 (9) (2005) 6177–6189, https://doi.org/10.4049/jimmunol.175.9.6177.

[25] R. Missiaen, F. Morales-Rodriguez, G. Eelen, P. Carmeliet, Targeting endothelial metabolism for anti-angiogenesis therapy: a pharmacological perspective, Vasc. Pharmacol 90 (2017) 8–18, https://doi.org/10.1016/j.vph.2017.01.001.

[26] L.A. Teuwen, N. Draoui, C. Dubois, P. Carmeliet, Endothelial cell metabolism: an update anno 2017, Curr. Opin. Hematol. 24 (3) (2017) 240–247, https://doi.org/10.1097/MOH.0000000000000335.

[27] Z. Dagher, N. Ruderman, K. Tornheim, Y. Ido, Acute regulation of fatty acid oxidation and amp-activated protein kinase in human umbilical vein endothelial cells, Circ. Res. 88 (12) (2001) 1276–1282, https://doi.org/10.1160/TH14-04-0360.

[28] S. Schoors, U. Bruning, R. Missiaen, K.C. Queiroz, G. Borgers, I. Elia, A. Zecchin, A.R. Cantelmo, S. Christen, J. Goveia, et al., Fatty acid carbon is essential for dNTP synthesis in endothelial cells, Nature 520 (7546) (2015) 192–197, https://doi.org/10.1038/nature 14362.

[29] K. De Bock, M. Georgiadou, P. Carmeliet, Role of endothelial cell metabolism in vessel sprouting, Cell Metab. 18 (5) (2013) 634–647, https://doi.org/10.1016/j.cmet.2013.08. 001.

[30] B.P. Dranka, B.G. Hill, V.M. Darley-Usmar, Mitochondrial reserve capacity in endothelial cells: the impact of nitric oxide and reactive oxygen species, Free Radic. Biol. Med. 48 (7) (2010) 905–914, https://doi.org/10.1016/j.freeradbiomed.2010.01.015.

[31] J. Deng, X. Liu, L. Rong, C. Ni, X. Li, W. Yang, Y. Lu, X. Yan, C. Qin, L. Zhang, et al., IFNγ-responsiveness of endothelial cells leads to efficient angiostasis in tumours involving down-regulation of Dll4, J. Pathol 233 (2) (2014) 170–182, https://doi.org/10.1002/path.4340.

[32] Ni C, Ma P, Wang R, Lou X, Liu X, Qin Y, Xue R, Blasig I, Erben U, Qin Z, et al. Doxorubicin-induced cardiotoxicity involves IFNγ-mediated metabolic reprogramming in cardiomyocytes. J. Pathol. 2018. DOI: https://doi.org/10.1002/path.5192.

[33] S.W. Shan, D.Y. Tse, B. Zuo, C.H. To, Q. Liu, S.A. McFadden, R.K. Chun, J. Bian, K.K. Li, T.C. Lam, et al., Data on differentially expressed proteins in retinal emmetropization process in Guinea pig using integrated SWATH-based and targeted-based proteomics, Data Brief 21 (2018) 1750–1755, https://doi.org/10.1016/j.dib.2018.08.119.

[34] U. Harjes, J. Kalucka, P. Carmeliet, Targeting fatty acid metabolism in cancer and endothelial cells, Crit. Rev. Oncol. Hematol 97 (2016) 15–21, https://doi.org/10.1016/j.critrevonc.2015.10.011.

[35] Y. Huang, R.W. Mahley, Apolipoprotein E: structure and function in lipid metabolism, neurobiology, and Alzheimer's diseases, Neurobiol. Dis 72 (Pt A) (2014) 3–12, https://doi.org/10.1016/j.nbd.2014.08.025.

[36] G. Velasco, M.J. Geelen, M. Guzmán, Control of hepatic fatty acid oxidation by 5'-AMP-activated protein kinase involves a malonyl-CoA-dependent and a malonyl-CoA-independent mechanism, Arch. Biochem. Biophys 337 (2) (1997) 169–175, https://doi.org/10.1006/abbi.1996.9784.

[37] D. Nagata, M. Mogi, K. Walsh, AMP-activated protein kinase (AMPK) signaling in endothelial cells is essential for angiogenesis in response to hypoxic stress, J. Biol. Chem 278 (33) (2003) 31000–31006, https://doi.org/10.1074/jbc.M300643200.

[38] M. Numasaki, J. Fukushi, M. Ono, S.K. Narula, P.J. Zavodny, T. Kudo, P.D. Robbins, H. Tahara, M.T. Lotze, Interleukin-17 promotes angiogenesis and tumor growth, Blood 101 (7) (2003) 2620–2627, https://doi.org/10.1182/blood-2002-05-1461.

[39] S.H. Chang, S.G. Mirabolfathinejad, H. Katta, A.M. Cumpian, L. Gong, M.S. Caetano, S.J. Moghaddam, C. Dong, T helper 17 cells play a critical pathogenic role in lung cancer, Proc. Natl. Acad. Sci. U. S. A 111 (15) (2014) 5664–5669, https://doi.org/10.1073/pnas.1319051111.

[40] A. Bezawork-Geleta, J. Rohlena, L. Dong, K. Pacak, J. Neuzil, Mitochondrial complex II: at the crossroads, Trends Biochem. Sci 42 (4) (2017) 312–325, https://doi.org/10.1016/j.tibs.2017.01.003.

[41] J. Pfleger, M. He, M. Abdellatif, Mitochondrial complex II is a source of the reserve respiratory capacity that is regulated by metabolic sensors and promotes cell survival, Cell Death Dis 6 (2015) e1835, https://doi.org/10.1038/cddis.2015.202.

[42] Z. Dagher, N. Ruderman, K. Tornheim, Y. Ido, The effect of AMP-activated protein kinase and its activator AICAR on the metabolism of human umbilical vein endothelial cells, Biochem. Biophys. Res. Commun 265 (1) (1999) 112–115, https://doi.org/10.1006/bbrc.1999.1635.

[43] J.A. Reihill, M.A. Ewart, I.P. Salt, The role of AMP-activated protein kinase in the functional effects of vascular endothelial growth factor-A and -B in human aortic endothelial cells, Vascular Cell 3 (2011) 9, https://doi.org/10.1186/2045-824X-3-9.

[44] R.F. Johnson, N.D. Perkins, Nuclear factor-κB, p53, and mitochondria: regulation of cellular metabolism and the Warburg effect[J], Trends Biochem. Sci 37 (8) (2012) 317–324, https://doi.org/10.1016/j.tibs.2012.04.002.

[45] C. Mauro, S.C. Leow, E. Anso, S. Rocha, A.K. Thotakura, L. Tornatore, M. Moretti, E. De Smaele, A.A. Beg, V. Tergaonkar, et al., NF-κB controls energy homeostasis and metabolic adaptation by upregulating mitochondrial respiration[J], Nat. Cell Biol 13 (10) (2011) 1272–1279, https://doi.org/10.1038/ncb2324.

[46] A.H. Remels, H.R. Gosker, K.J. Verhees, R.C. Langen, A.M. Schols, TNF-α-induced NF-κB activation stimulates skeletal muscle glycolytic metabolism through activation of HIF-1α[J], Endocrinology 156 (5) (2015) 1770–1781, https://doi.org/10.1210/en.2014-1591.

[47] M. Saito, M. Saito, B.C. Das, Involvement of AMP-activated protein kinase in neuroinflammation and neurodegeneration in the adult and developing brain[J], Int. J. Dev. Neurosci (2019), https://doi.org/10.1016/j.ijdevneu.2019.01. 007 pii: S0736-5748(18)30276-4.

[48] S. Giri, N. Nath, B. Smith, B. Viollet, A.K. Singh, I. Singh, 5-aminoimidazole-4-carboxamide-1-beta-4-ribofuranoside inhibits proinflammatory response in glial cells: a possible role of AMP-activated protein kinase[J], J. Neurosci 24 (2) (2004) 479–487, https://doi.org/10.1523/JNEUROSCI.4288-03.2004.

[49] S.Y. Park, M.H. Choi, M. Li, K. Li, G. Park, Y.W. Choi, AMPK/Nrf2 signaling is involved in the anti-neuroinflammatory action of Petatewalide B from Petasites japonicus against lipopolysaccharides in microglia[J], Immunopharmacol. Immunotoxicol 40 (3) (2018) 232–241, https://doi.org/10.1080/08923973.2018.1434791.